ELSEVIER

*Dyes and Pigments*, Vol. 36, No. 1, pp. 35–43, 1998

PII: S0143-7208(96)000125-8 0143-7208/97 $17.00+0.00

# Spectral Properties of Tetrathiabenzoquinones and Their Self-assembly in the Solid State

Koichi Takagi,[a] Akira Mizuno,[a] Akihiro Iwamoto,[a†] Masaru Furusyo[a‡] & Masaru Matsuoka[b]

[a]Department of Industrial Chemistry, Wakayama National College of Technology, Gobo, Wakayama 644, Japan
[b]Laboratory of Material Science, Kyoto Women's University, Imakumano, Higashiyama-ku, Kyoto 605, Japan

(Received 17 October 1996; accepted 19 November 1996)

*ABSTRACT*

*Bis(1,4-dithiacyclohexano)[2,3-b:2',3'-e]-1,4-benzoquinone* **3a** *and analogous cyclic dithiaquinone derivatives were synthesized. The difference* ($\Delta\lambda$) *in* $\lambda max$ *of these dyes between the solution phase and vapor deposited thin film indicates the degree of strength of the intermolecular* $\pi$–$\pi$ *interactions in the solid state. The* $\Delta\lambda$ *values were largely affected by the interlayer distances and the steric requirements of the molecules. The three dimensional molecular stacking of dye* **3a** *was evaluated by X-ray crystal analysis and the substituent effects on the properties of analogous dyes were evaluated by the MOPAC and AMPAC calculation methods. The vapor deposited thin film of dye* **3a** *gave large 3rd order nonlinear optical susceptibility. The intermolecular* $\pi$–$\pi$ *interactions of the dye molecules play an important role for these special functionalities.* © *1997 Elsevier Science Ltd*

*Keywords*: Tetrathiabenzoquinone, Solid state absorption spectra, Vapor deposited thin film, Intermolecular $\pi$–$\pi$ interactions, 3rd Order NLO material, AMPAC calculation.

## INTRODUCTION

Many functionalities of organic materials are induced by $\pi$-electron oriented intermolecular interactions. Molecular interactions, including $\pi$–$\pi$ interac-

†Present address; R & D Group, Special Compounds & Colorants Division, DIC Inc., Nishiki, Warabi, Saitama 335, Japan.
‡Present address; CAE Research Center, Sumitomo Electic Co., Ltd., Hikaridai, Seika, Soraku, Kyoto 619-02, Japan.

tions and the nature of the molecular stacking, are the most important factors with respect to special functionalities. The solid state chemistry of dye molecules is of current interest, particularly in correlating their functionality with structure in the solid state, with regard to functional materials such as organic nonlinear optical (NLO) materials, organic photoconductors (OPC), emitters for electroluminescence (EL), etc. Dye molecules generally have large $\pi$–conjugated planar structure and are valuable candidates for organic functional materials [1]. Many functionalities are due to the intra- and intermolecular $\pi$–$\pi$ interactions of dye molecules in solid state.

We have reported that symmetrical 2,6-(bis-butylamino)naphthazarin showed strong three dimensional molecular stacking caused by the intermolecular hydrogen bonding and the interlayer interactions which produced a large bathochromic shift ($\Delta\lambda = 100$ nm) of absorption maximum in vapor deposited thin film, and gave large 3rd order nonlinear optical susceptibility. On the other hand, asymmetrical 2-butylaminonaphthazarin did not show any special characterizations. These compounds are similar in their chemical structure and show similar absorption spectra in solution, but quite different spectra in the solid state [2, 3]. Comparison of these characterizations with respect to intermolecular $\pi$–$\pi$ interactions and molecular stacking is, therefore, of interest.

We designed new types of quinone dyes which perform three dimensional molecular stacking caused by the intermolecular $\pi$–$\pi$ interactions. Tetrathiabenzoquinone dyes have a strong intramolecular charge-transfer chromophoric system in which the sulfur atoms act as donor moieties and the quinone groups act as acceptors. On the other hand interlayer $\pi$–$\pi$ interactions of charge-transfer character is also expected in the chromophore, playing a significant role in the three dimensional molecular stacking.

We have now synthesized symmetrical and asymmetrical cyclic thiaquinone dyes by the known synthetic method [4, 5], and evaluated their spectral properties both in solution and vapor deposited thin film. The difference in absorption maximum ($\Delta\lambda$) was correlated with their intermolecular interactions in the solid state by X-ray crystal analysis and the molecular orbital calculation method.

## RESULTS AND DISCUSSION

### Syntheses of cyclic thiaquinones

The reaction of tetrachlorobenzoquinone 1 with dithiols **2a-2d** in the presence of sodium carbonate gave the symmetrical cyclic tetrathiabenzoquinones (**3a-3d**) in moderate yields [4, 5]. Similar reaction of 1 with 2-hydroxylethanethiol **2e** gave **3e**, the oxygen analogue of **3a** in 21% yield. On the other

hand, the reaction of 2,3-dichloronaphthoquinone **4** with **2** gave the corresponding asymmetrical cyclic dithianaphthoquinones **5** in better yield [4,5]. Reactions giving the cyclic thiaquinones are shown in Scheme 1. The absorption spectra of these dyes in chloroform solution and vapor deposited thin film, together with the $\Delta\lambda$ values are summarized in Table 1.

## Absorption spectra of dyes in solution and solid state

It is generally known that the solid state $\lambda$max value of a dye shifts to longer wavelength, by around 30–80 nm, compared with that in solution, due to the stronger molecular interaction in the solid state [6]. Solid state absorption spectra of some dyes have been reported which showed a large bathochromic shift of $\lambda$max caused by strong intermolecular $\pi$–$\pi$ interactions [3, 7].

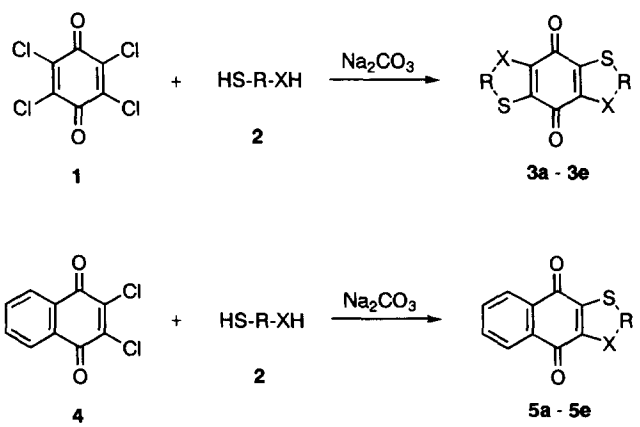


R and X are indicated in Table 1

**Scheme 1.**

**TABLE 1**
Absorption Spectra of Dyes **3** and **5** in Solution and Solid State

| *Dye* | *R* | *X* | *Yield (%)* | *λmax (log ε) (nm)*[a] | *λmax (nm)*[b] | *Δλ (nm)* |
|---|---|---|---|---|---|---|
| **3a** | $-(CH_2)_2-$ | S | 54 | 429(4.0), 590(2.0) | 538 | 109 |
| **3b** | $-(CH_2)_3-$ | S | 82 | 454(3.9), 605(2.0) | 503 | 49 |
| **3c** | 1,2-Phenyl- | S | 53 | 517(2.7), __[c] (__[c]) | 587 | 70 |
| **3d** | $-CH(CH_3)CH_2-$ | S | 62 | 431(4.0), 581(2.3) | 460 | 29 |
| **3e** | $-(CH_2)_2-$ | O | 21 | 379(4.2), 552(2.8) | 420 | 41 |
| **5a** | $-(CH_2)_2-$ | S | 87 | 495(3.4) | 547 | 52 |
| **5b** | $-(CH_2)_3-$ | S | 82 | 516(3.4) | 535 | 19 |
| **5c** | 1,2-Phenyl | S | 84 | 542(2.7) | — | — |
| **5e** | $-(CH_2)_2-$ | O | 42 | 454(3.2) | 475 | 21 |

[a]in $CHCl_3$; [b]solid; [c]the corresponding n–$\pi^*$ transition was not observed.

The principal absorption spectra of tetrachlorobenzoquinone 1 in solution was observed at 375 nm but dye **3a** absorbed at around 430 nm. Introduction of the sulfur bridges as donor moieties produced a bathochromic shift of 54 nm from **1** to **3a**. Extension of $\pi$– conjugation by the phenyl groups in **3c** produced a large bathochromic shift of 89 nm from **3a** to **3c**, but the corresponding $n$–$\pi^*$ transitions observed at 590 nm in **3a** disappeared. These observations were well explained by the MO method, in which the calculated oscillator strength (f) of the $n$–$\pi^*$ transition for **3c** was zero (Table 2). Similar longer wavelength $\pi$–$\pi^*$ absorption at 542 nm was also observed in dye **5c**. The origin of the longer wavelength $n$–$\pi^*$ absorption of dyes **3** was due to the transition from the nonbonding electrons of the sulfur atoms to the lowest $\pi^*$ orbital, because their molecular absorptivity ($\varepsilon$) were very small (values of several hundred). The $\varepsilon$ value of the first $\pi$–$\pi^*$ transition of these dyes were rather small, around $10^4$ because of their small $\pi$–conjugation system. The oxygen analogues (**3e** and **5e**) absorbed at shorter wavelength region compared with the sulfur analogues. This is caused by the weaker electron donating ability of the oxygen atom compared with that of the sulfur atom.

On the other hand, solid state absorption spectra indicated that the shape of absorption curves was very similar to that in solution, but the λmax shifted to longer wavelength depending on their chemical structures (Fig. 1). Relevant λvalues are shown in Table 1. The Δλ value of dye **3a** was 109 nm, and those of the others were **3b** (49 nm), **3c** (70 nm), **3d** (29 nm), and **3e** (41 nm). Dye **3a** showed an exceptionally large Δλ value compared to the other dyes and dye **3c** also showed a quite large Δλ value but dye **3d** showed a small value. On the other hand, the Δλ values of the oxygen analogues **3e** and **5e** were less than half those for the sulfur derivatives **3a** and **5a**, because of the lower electron donating ability of the oxygen atoms or the lower symmetry of their structures. In dyes **5**, only dye **5a** showed a significant Δλ value (52 nm). From these observations, we can say that the symmetrical dyes **3** showed larger Δλ values compared with the corresponded asymmetrical dyes **5**, and that molecular symmetry is very necessary for strong molecular stacking. The substituent effects of dyes **3a**, **3b** and **3d** on their conformational structures were simulated by using the MOPAC calculation method.

**TABLE 2**
Calculated Absorption Spectra of Dyes **3a** and **3c** by the AMPAC PM3 Method

| *Dye No.* | *λmax (nm)* | *f* | *Transition* |
|---|---|---|---|
| | 445.6 | 0.007 | n–π* |
| **3a** | 376.3 | 0.4847 | π–π* |
| | 537.0 | 0.0000 | n–π* |
| **3c** | 481.5 | 0.1099 | π–π* |
| | 453.7 | 0.0463 | π–π* |

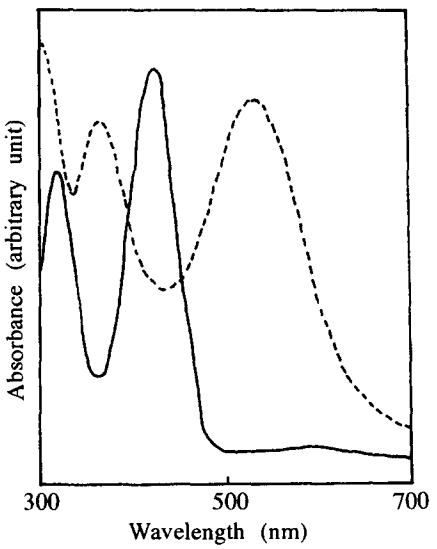


**Fig. 1.** Absorption spectra of **3a** in chloroform solution (solid line) and vapor deposited thin film (broken line).

## Conformational analyses of dye 3 by the MOPAC PM3 method

The structure of dyes **3a**, **3b** and **3d** were optimized by the MOPAC PM3 method and these results are shown in Fig. 2. Dye **3a** has a planar structure in a $\pi$–conjugated moiety, but has some "bent" structure in the six membered aliphatic moiety caused by the $sp^3$ hybridization of the ethylene carbons. The structural optimization of dye **3a** using *ab-initio* calculation of Gaussian 94W (6–31G**) [9] indicated that the deviation of the alkyl chain from the $\pi$–plain was around 0.47 Å. These results were also confirmed by X-ray crystal analysis on the solid state as indicated in the following section. On the other hand dye **3b** also has a planar $\pi$–conjugation, but the sulfur atoms deviated somewhat from the quinone moiety. The seven membered alkyl rings deviated largely compared with those of dye **3a**. It is proposed that dye **3b** has some difficulties for molecular stacking by intermolecular $\pi$–$\pi$ interactions because of steric hindrance factors. On the other hand dye **3d**, as dye **3a**, has quite a planar structure, but the methyl group attached to the six membered alkyl ring oriented to the direction of the longer molecular axis occupies a large space, thus preventing molecular stacking due to this steric hindrance of the methyl group. It is generally known that molecular packing to get higher density in the solid state, should be performed to occupy the smallest space, and the space-occupying methyl substituents are unfavorable for intermolecular $\pi$–$\pi$ interactions. From these

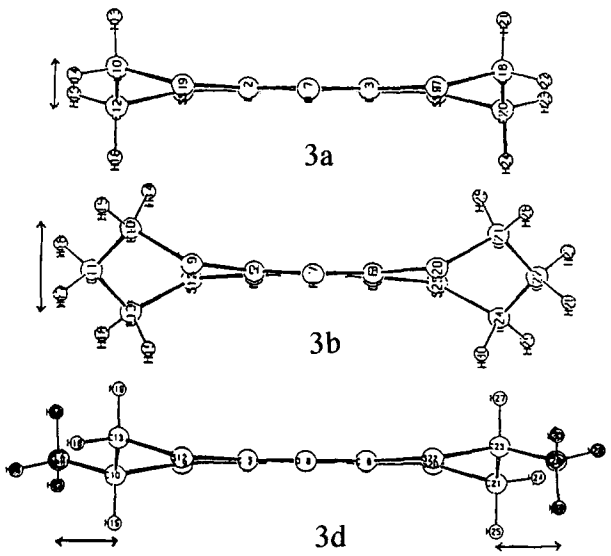


**Fig. 2.** Optimized structures of **3a**, **3b** and **3d** by MOPAC PM3 method.

results, we can evaluate the substituents effects of molecular stacking of these dyes by means of the MOPAC method. The $\Delta\lambda$ value shown in Table 1 well reproduced these result, viz., the larger the $\Delta\lambda$ value, the stronger the interlayer $\pi$–$\pi$ interactions.

## X-ray crystal analysis of dye 3a

A single crystal of dye **3a** was obtained from toluene solution as dark red colored cubic crystals. X-ray crystal analysis was performed in Mac Science. Results are summarized in Table 3. The crystal system of 3a is orthorhombic and it belongs to the Iba2 space group. Each molecule aligns in the same plane and overlaps perpendicular along with the quinone ring. Figure 3 showed the projection of the crystal structure on the (b,c) plane. The molecules are stacked in a herringbone fashion along the a axis with an interplanar distance of 3.6 Å. Strong interlayer $\pi$–$\pi$ interactions are estimated from this distance, and the electrostatic dipole repulsion of the carbonyl groups may control the perpendicular overlap of each molecule in the nearest upper and lower layers. The molecules stacked to form columns, as shown in Fig. 3a; the molecular alignments in the unit cell are shown in Fig. 3b. It is of interest to note that molecular overlap occurred so as to get the best $\pi$–$\pi$ interactions in the $\pi$–plane and to avoid the steric hindrances of the alkyl rings. The interlayer distance of 3.6 Å strongly indicates that the $\pi$–$\pi$ interactions

**TABLE 3**
Crystal Data of **3a**

| | | |
|---|---|---|
| Formula | | $C_{10}H_8O_2S_4$ |
| Formula Weight | | 288.40 |
| Crystal System | | Orthorhombic |
| Space Group | | Iba2 |
| Cell Dimension | a/Å | 9.444(2) |
| | b/Å | 16.593(4) |
| | c/Å | 7.196(2) |
| | V/Å$^3$ | 1127.8(4) |
| Z | | 4 |
| D/g cm$^{-3}$ | | 1.70 |
| Residuals, R | | 0.0548 |
| Residuals, Rw | | 0.0492 |
| Reflections used | | 471 |

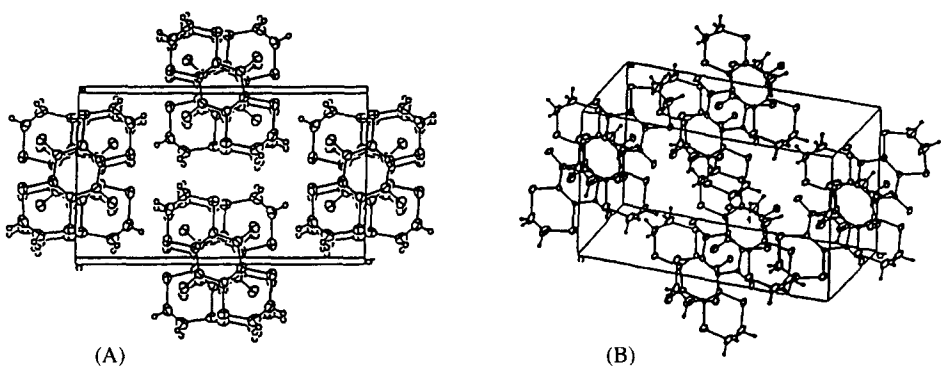


**Fig. 3.** X-ray crystal structure of **3a**; molecular overlap view from the c-axis (A) and from the (a,b) plane (B).

played a large role in controlling the molecular packing, and gave the large λ value in solid state absorption spectra, and the large $\chi^3$ value necessary for NLO materials.

## Experimental

All melting points are uncorrected. Visible spectra in chloroform solution were recorded on a Hitachi EPS-3T spectrophotometer. $^1$H-NMR spectra were recorded on a Varian Unity-plus 300 NMR spectrometer in $d_6$-DMSO solution with tetramethylsilane as internal reference. Elemental analyses were recorded on a Yanaco CHN Corder MT-3. Column chromatography was carried out on silica gel (Wakogel C-300) using appropriate solvents. Molecular orbital calculations were conducted by using AMPAC version 5 with key words MECI under configuration interaction number of 10 in the

PM3 method. Conformational analyses were conducted using the MOPAC PM3 [10] method.

## MATERIALS

Thiaquinone derivatives **3** and **5** were prepared by the previously reported method [5]. Reagents **1**, **2** and **4** were commercial grade and were used without further purification.

### Synthesis of 3a (general procedures)

2,3:5,6-Bis(ethylenedithio)-1,4-benzoquinone (**3a**) was prepared by refluxing a mixture of chloranil **1** (1.0 g, 4 mmol), sodium carbonate (3.9 g, 37 mmol), and 1,2-ethanedithiol **2** (0.89 g, 9.5 mmol) in ethanol (500 ml) under argon atmosphere for 5 h. The mixture was concentrated in *vacuo*, and the residue was extracted with dichloromethane using a Soxhlet extractor. After evaporation in *vacuo*, the residue was recrystallized from chlorobenzene to give green colored fine crystals of **3a** in 54 % yield.

### Characterization and identification of products

Compounds **3a**, **3b**, **5a** and **5b** are known and were identified by the data described in the literature [5]; relevant characterization data is given below.

**3a**; mp $>300°C$, $^1H$–NMR $\delta = 3.28$(s), MS m/z($M^+$) = 288.

**3b**; mp $>300°C$, $^1H$–NMR $\delta = 2.00$(q, 4H, J = 6.0 Hz), 3.51(t, 8H, J = 6.0 Hz), MS m/z ($M^+$) = 316.

**3c**; mp 352–354°C, MS m/z($M^+$) = 384, Anal. Calcd. for $C_{18}H_8O_2S_4$, C = 56.25, H = 2.10, Found, C = 56.22, H = 1.88.

**3d**; mp 261–263°C, MS m/z($M^+$) = 316, $^1H$–NMR $\delta = 1.37$(d, 6H, J = 6.6 Hz), 3.03(dd, 4H, J = 13.4, 6.9 Hz), 3.59(m, 2H), Anal. Calcd. for $C_{12}H_{12}O_2S_4$, C = 45.57, H = 3.80 Found, C = 45.88, H = 3.91.

**3e**; mp 325–330°C(dec.), MS m/z($M^+$–1) = 255, $^1H$–NMR $\delta = 3.15$(m, 4H), 4.39(m, 4H), Anal. Calcd. for $C_{10}H_8O_4S_2$, C = 46.88, H = 3.13, Found, C = 46.64, H = 3.12.

**5a**; mp 241–242°C, $^1H$–NMR $\delta = 3.31$(s, 4H), 7.69(dd, 2H, J = 5.7 Hz, 3.0 Hz), 8.07(dd, 2H, J = 5.7 Hz, 3.0 Hz), MS m/z($M^+$) = 248.

**5b**; mp 151–152°C, MS m/z($M^+$) = 262.

**5c**; mp 274–275°C, MS m/z($M^+$) = 296, Anal. Calcd. for $C_{14}H_8O_2S_2$, C = 46.88, H = 3.13, Found, C = 47.02, H = 3.25.

**5e**; mp 222–223°C, MS m/z($M^+$) = 232, $^1H$–NMR $\delta = 3.18$(dd, 2H, J = 6.0, 4.5 Hz), 4.59 (dd, 2H, J = 6.0, 4.5 Hz), 7.67–7.72(m, 2H), 8.01–8.13(m, 2H), Anal. Calcd. for $C_{12}H_8O_3S$, C = 62.07, H = 3.45, Found, C = 62.33, H = 3.24.

## ACKNOWLEDGEMENTS

The X-ray crystal analysis was conducted by Miss. A. Nakao in Mac Science. Part of the MOPAC calculations were carried out by Dr. H. Shiozaki in the Osaka Prefectural Industrial Technology Research Institute. The authors are greatly indebted to their help. This work was partially supported by the Grant-in-Aid for Scientific Research from the Ministry of Education, Science and Culture (Nos 07241259, 07246238 and 08236232).

## REFERENCES

1. Matsuoka, M., *J. Soc. Dyers Colourists*, **105** (1989) 167.
2. Matsuoka, M., Oshida, A., Mizoguchi, A., Hattori, Y. and Nishimura, A., *Nonlinear Optics*, **10** (1995) 109.
3. Kim, J. H., Matsuoka, M. and Fukunishi, K., *Dyes and Pigments*, **31** (1996) 263.
4. Hahn, W. E. and Wojciechowski, L., *Rocz, Chem.*, **41** (1967) 1067.
5. Otsubo, T., Nobuhara, Y., Kanefuji, K., Aso, Y. and Ogura, F., *J. Phys. Org. Chem.*, **1** (1988) 275.
6. Matsuoka, M., Saitoh, Y., Oka, H. and Kitao, T., *Koubunshi Ronbunsyu*, **47** (1990) 875.
7. Mizuguchi, J. and Wooden, G., *Ber. Bunsenges. Phys. Chem.*, **95** (1991) 1264.
8. Mizuguchi, J., Rochat, A. C. and Rihs, G., *ibid*, **96** (1992) 607.
9. Furusyo, M. and Matsuoka, M. unpublished results.
10. MOPAC Ver. 6, J. J. P. Stewart, QCPE #455; Revised as Ver. 6.01 by T. Hirano, *JCPE Newsletter*, **2** (1991) 26.